

LASER INTERFEROMETER GRAVITATIONAL WAVE OBSERVATORY
- LIGO -

=====

LIGO SCIENTIFIC COLLABORATION

| | | |
|--|--------------------------|------------|
| Technical Note | LIGO-T1400513-v1- | 2014/09/20 |
| Silicon Cantilevers Report II | | |
| Marie Lu, Nic Smith, Rana Adhikari, Zach Korth | | |

California Institute of Technology
LIGO Project, MS 18-34
Pasadena, CA 91125
Phone (626) 395-2129
Fax (626) 304-9834
E-mail: info@ligo.caltech.edu

Massachusetts Institute of Technology
LIGO Project, Room NW22-295
Cambridge, MA 02139
Phone (617) 253-4824
Fax (617) 253-7014
E-mail: info@ligo.mit.edu

LIGO Hanford Observatory
Route 10, Mile Marker 2
Richland, WA 99352
Phone (509) 372-8106
Fax (509) 372-8137
E-mail: info@ligo.caltech.edu

LIGO Livingston Observatory
19100 LIGO Lane
Livingston, LA 70754
Phone (225) 686-3100
Fax (225) 686-7189
E-mail: info@ligo.caltech.edu

Contents

| | |
|--|-----------|
| Introduction | 2 |
| Methods of Determining the Quality Factor | 3 |
| Clamp Models | 5 |
| Designing the Experiment | 5 |
| Measurements on Aluminum | 6 |
| Planning Ahead | 6 |
| Figures | 7 |
| Tables | 16 |
| Works Cited | 16 |

Introduction

Originally proposed in 1916 as a part of the theory of general relativity, gravitational waves and their detection have been a major investment for many scientists. LIGO, the Laser Interferometer Gravitational-Wave Observatory, measures ripples in the force of gravity emitted from major cosmic events. The LIGO detector is a Michelson interferometer, composed of a series of fixed silica mirrors suspended from fibers in a pendulum. Because gravitational waves are incredibly weak, it is necessary to reduce noise sources as much as possible in order to obtain accurate results. Currently, the material for the wires–fused silica– still contributes significant thermal noise uniformly across the noise floor, preventing the detectors from reaching their quantum mechanical sensitivity limits. Our research will focus an alternative material, silicon, for the fibers that has lower thermal fluctuations. This material will likely operate under cryogenic temperatures to minimize the mechanical dissipation of atoms vibrating from thermal fluctuations.

In reality, thermal fluctuations are incredibly small and hard to measure accurately. So instead, the fluctuation dissipation theorem allows us to measure the mechanical dissipation of a material, which is directly related to the amount of thermal fluctuations. To derive one from the other, we start with the equation of motion of the particles inside a material modeled by

$$\ddot{x} = -\omega_0^2(1 + i\phi)x + F \quad (1)$$

where ϕ is the loss angle:

$$\phi = \Delta \frac{\omega\tau}{1 + \omega^2\tau^2} \quad (2)$$

Another parameterization of this equation can be obtained by replacing the complex component with a variable γ , resulting in

$$\ddot{x} = -\omega_0^2x - \gamma\dot{x} + F \quad (3)$$

where $\gamma = \frac{\omega_0^2\phi}{\omega}$, which we find from setting the two different parameterizations equal to each other. This results in the the power spectrum of the motion of the mass

$$x^2(\omega) = \frac{4k_B T \sigma(\omega)}{\omega^2} \quad (4)$$

with $\sigma(\omega)$ denoting the mechanical conductance, which is also the real part of the admittance:

$$Y(\omega) = \frac{\omega\phi + i(\omega - m\omega^3)}{(k - m\omega^2)^2 + k^2\phi^2} \quad (5)$$

Solving for $\sigma(\omega)$ and substituting into Equation 4 produces the power spectral density of the position of the mass:

$$x^2(\omega) = \frac{4k_B T k \phi(\omega)}{\omega[(k - m\omega^2)^2 + k^2\phi^2]} \quad (6)$$

Thus, in order to map out the noise spectrum, our experiments measure ϕ , a quantity that is inversely proportional to the quality factor of the material, as we will show later.

Methods of Determining the Quality Factor

The first method is the ringdown technique, which consists of driving the cantilever at resonance, removing the driving force, and recording the exponentially damped oscillations. If we start at the equation of motion (Equation 3) and solve for the transfer function, we see that the quality factor is directly proportional to the time constant. Setting \bar{x} and \bar{F} as the Laplace transforms of x and F , respectively, we take the Laplace transform of both sides of our equation of motion, giving

$$s^2\bar{x} = -\omega_0^2\bar{x} - \gamma s\bar{x} + \bar{F} \quad (7)$$

Solving for $\frac{\bar{x}}{\bar{F}}$ produces the transfer function:

$$\begin{aligned} \frac{\bar{x}}{\bar{F}} &= \frac{1}{s^2 + \gamma s + \omega_0^2} \\ &= \frac{1}{(s + \frac{\gamma}{2})^2 + (\omega_0^2 - \frac{\gamma^2}{4})} \\ &= \frac{\sqrt{\omega_0^2 - \frac{\gamma^2}{4}}}{(s + \frac{\gamma}{2})^2 + (\omega_0^2 - \frac{\gamma^2}{4})} \frac{1}{\sqrt{\omega_0^2 - \frac{\gamma^2}{4}}} \end{aligned}$$

Now we take the inverse Laplace transformation to obtain the impulse function:

$$I(t) = e^{-\frac{\gamma}{2}t} \sin \sqrt{\omega_0^2 - \frac{\gamma^2}{4}}t \quad (8)$$

We may make the approximation that $\frac{\gamma}{\omega_0}$ is small, making $\frac{\gamma^2}{4}$ is negligible compared to ω_0^2 :

$$I(t) = e^{-\frac{\gamma}{2}t} \sin \omega_0 t \quad (9)$$

This is a damped sinusoid with a time constant $\tau = \frac{2}{\gamma} = \frac{2\omega}{\omega_0^2\phi}$

By definition, the quality factor is

$$Q \equiv \frac{\omega_0}{\Delta\omega} \quad (10)$$

where $\Delta\omega$ is the bandwidth, or, the full width at half max of the peak centered at the resonant frequency of the transfer function. Because τ is the time it takes for the wave to decay to $\frac{1}{e}$ of the original power, in frequency space we can observe that $2\frac{1}{\tau} = \Delta\omega$ so then $Q = \frac{\omega_0\tau}{2}$. Thus from the ringdown experiment, we can obtain τ and thus Q .

Furthermore, if we substitute $\tau = \frac{2\omega}{\omega_0^2\phi}$ into $Q = \frac{\omega_0\tau}{2}$, then

$$Q(\omega) = \frac{\omega}{\omega_0\phi} \quad (11)$$

Evaluating this expression at ω_0 , gives $Q = \frac{1}{\phi}$. Thus by measuring the time constant from the decaying sinusoid of the cantilever, we can find the quality factor and the needed value of ϕ for the noise spectrum (Equation 6).

The second method is to drive the oscillator with white noise and to study the cantilever's transfer function. Again, from the definition of $Q = \frac{\omega_0}{\Delta\omega}$, we can look at the transfer function of the cantilever's motion and fit a Lorentzian curve to the peak at the resonant frequency, thus obtaining the value of the resonant frequency and the bandwidth to calculate Q and ϕ .

However both of these experiments have impracticalities in execution. The first method is applied with the assumption that the driving frequency is exactly at the resonant frequency with an accuracy of at least one part in Q . This can be difficult in practice. In addition, the ringdown time in the first method can be several hours, presenting another practical concern. Lastly, we assumed in both of the previous methods that the measurement of Q is independent of the driving amplitude. However, a greater drive may increase the friction within the clamp and contribute complicated damping to the system that will confuse our measurements of Q .

This final method addresses these issues. This design (See Figure 6) uses two control loops to keep the driving force locked to the natural resonant frequency and to lock the oscillator at a fixed oscillation amplitude. The phase locked loop (PLL) is achieved by making the auxiliary oscillator a voltage controlled oscillator (VCO) that is locked to the signal of the position output. The amplitude locked loops is comprised of an amplitude detector which is then compared to a reference amplitude. The error signal is amplified and used to adjust the strength of the drive.

To see how this method measures the quality factor, we will focus on the output of the amplitude control output and the amplitude amplitude set point, which we will call a and c respectively. We will also do our analysis referring to the linearized model of the ALL (Refer to Figure 7). Then,

$$\frac{a}{c} = \frac{H}{1 + G} \quad (12)$$

$$= \frac{H\phi\omega_0(1 + i\tau\omega)}{(\phi\omega_0 + \frac{SHA}{\omega_0})(1 + \frac{2i\omega}{\phi\omega_0} + \frac{SHA}{\omega_0})} \quad (13)$$

If we take the limit of high gain and solve for ϕ , we arrive at

$$Q = \phi^{-1} = \left(\frac{2\omega_U}{cH_U\omega_0}\langle a \rangle\right)^{-1}. \quad (14)$$

where $\omega_U = \frac{|SHA|}{2\omega_0}$ is the unity gain frequency and H_U is the gain of H at the unity gain frequency.

With this implementation, Q is can be calculated continuously and instantaneously from the information used to maintain the control loops, which is an advantage over the ringdown

technique, which may take up to several hours to complete. In addition, all of the Q measurements from this process are made at a constant, chosen amplitude. Thus, we can control the amplitude to determine how Q depends on drive amplitude, possibly giving indications on the amount of clamp loss present. This could be useful if we wish to improve the clamp design in the future.

Clamp Models

Before we make any measurements of the thermal dissipation of our silicon wafer, we must design an experimental set-up. In particular, we need to find a clamp structure to hold the silicon test mass that minimizes the amount of clamping loss. The silicon cantilevers are etched out of whole silicon wafer (See Fig 1 for reference). The clamp will hold the wafer on either side, at the center, secured by a screw that will pass through the center hole. Initially, we hypothesized that reducing the area of contact between the silicon wafer and the steel clamp components would lessen the clamp loss. Thus we played with model shapes that would test this factor.

Here are the three major clamp designs that we focused on:

- Model 1: The clamp is composed of two solid cylinders on either side of the wafer held in place by a screw.
- Model 2: Two cylindrical disks, one on either side of the wafer, are supported on four hemispheres, making contact with the silicon surface at only four points on each side of the wafer. The four contact points form a square.
- Model 3: Two solid cylinders, one on either side of the wafer, with the center of the cylinders are hollowed out such that there is only a ring of contact between the steel clamp and the wafer.

We found that a Model 1 clamp with a 6 mm radius produced the best strain energy ratio. Models 1 and 3 produced strain energy ratios that were 2 orders of magnitude better than that produced by Model 2. Thus we will focus on Models 1 and 3 in this discussion. Shortening the radii allowed for smaller clamp loss in both designs (Refer to Figure 4 for a plot of strain energies over the eigenfrequencies). Although Model 3 has lower strain energy ratios at eigenfrequencies below approximately 245 Hz, our experiment mainly pertains to eigenmodes of the rectangular cantilevers on the wafer, which are from 251 to 298 Hz. This is where Model 1 consistently produced lower strain energy than Model 3, although the two are close.

Designing the Experiment

Based on the constraints of the model we developed, we then drafted a experimental set-up in SolidWorks. See Figure 5 for details on the design. The silicon cantilever is excited

into oscillatory motion by an electrostatic driver (ESD) and an optical lever captures the motion. A helium neon laser enters through a slit centered between the spacers holding up the ESD, bounces off of the 45 degree mirror onto the oscillating cantilever above, and back onto the mirror and out of the slit. The signal is detected by a quadrant photodiode (QPD). As the cantilever moves up and down, the angle of reflection of the beam will change, and we observe the oscillating behavior and calculate the quality factor with the three different methods described above. There is a power resistor to control the temperature. Liquid nitrogen at the base of the assembly keeps the system cool to a minimum of 77 K. However, if we wish to raise the temperature, the power resistor provides heat. The insulating layer beneath the clamp is used to keep the heat from flowing out into the liquid nitrogen too quickly if we choose to apply heat. A small resistor placed in the groove of the bottom clamp will sense the temperature. The entire system is under vacuum.

Measurements on Aluminum

While we have been waiting for the parts of our experimental setup to arrive from the machine shop, we made practice measurements of Q on aluminum sham cantilevers using the old experimental design. (See Table 1 for summary of results.) With the data from the ringdown method, we extracted the peak points of the decaying wave with a Python function that identifies local extrema and curve fitted the points to

$$y = Ae^{-Bt} + C \quad (15)$$

Using this technique, we found an average Q of 363 ± 1 .

For the transfer function method, we fitted a Lorentzian with a linear term to the Laplace transform of the timestream data:

$$y = \frac{A}{B^2 + (x - \omega_0)^2} + mx + C \quad (16)$$

By definition, $x = (\omega_0 \pm \frac{1}{2}B)$ is the position of the half maximum. Thus from our curve fit, we obtained $\Delta\omega$ and ω_0 , allowing us to calculate Q . We believe there is a linear term in our data due to noise possibly. However, the level is so very low ($m \approx 1 \times 10^4$) and is not a large source of error in measuring Q .

We found that the Q was 246 ± 4.92 . See Figures 8 and 9 for examples of our fits. For each of our tests, we found the error by using the covariance matrix produced by the Python curvefit function and error propagation:

$$s_Q^2 = \sum_{i=1}^N \left(\frac{\partial A}{\partial x_i} \right)^2 s_{x_i}^2 \quad (17)$$

and N is the number of variables that Q depends on, s_Q is the standard deviation of Q , and s_{x_i} is the standard deviation of each variable x_i . While this old set up does not give an accurate Q value due to high clamp losses, we do see consistency with among the results which indicates that our theory has good backup, but that we are limited by systematic issues that we expect our new clamp to eliminate.

Planning Ahead

The parts that we ordered from the manufacturer's have just arrived. We have spent the past few days putting the parts together and aligning the laser. We are currently working on programming the temperature control system. Once that is complete, we will begin testing the silicon cantilevers immediately as a function of frequency, drive amplitude, and temperature. We will apply all three methods described above to check for consistency. If time permits, we will then consider testing the silicon under various surface treatments, such as thin films, etching, or doping.

Figures

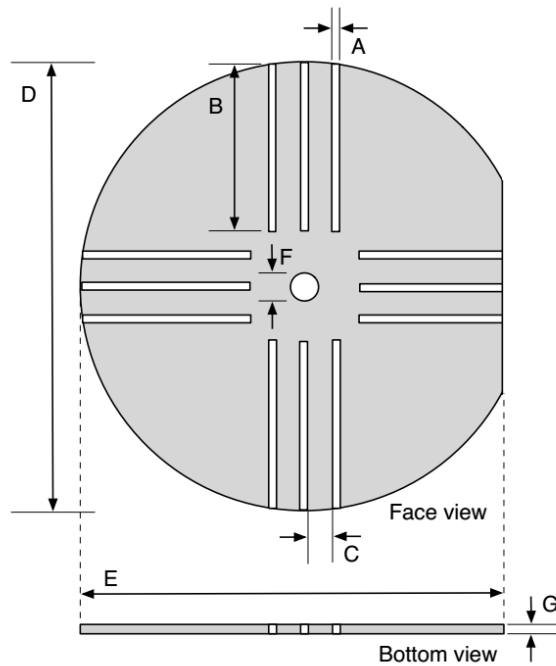


Figure 1: $A = 1.5$ mm, $B = 34$ mm, $C = 10$ mm, $D = 100$ mm (as per their info), $E = (100 - X)$ mm, where $X =$ flat sagitta (yet to be specified), $F = 10$ mm, $G = 0.3$ mm

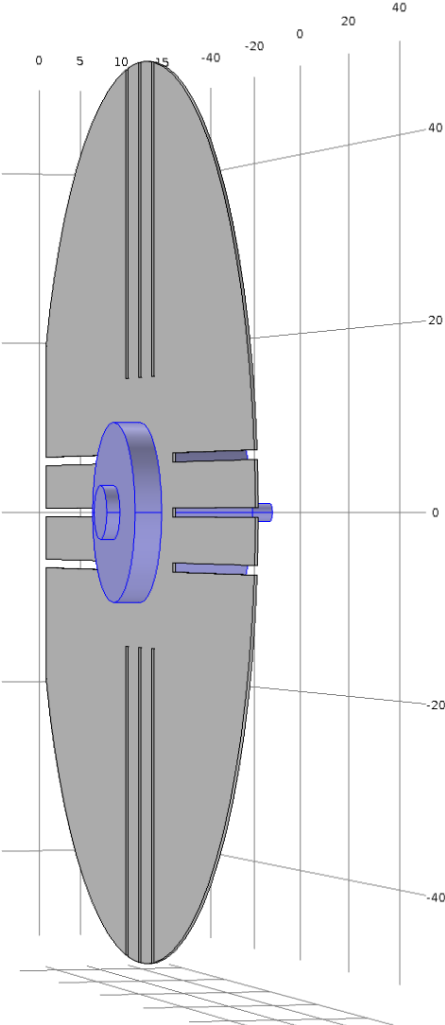


Figure 2: Model 1, front view

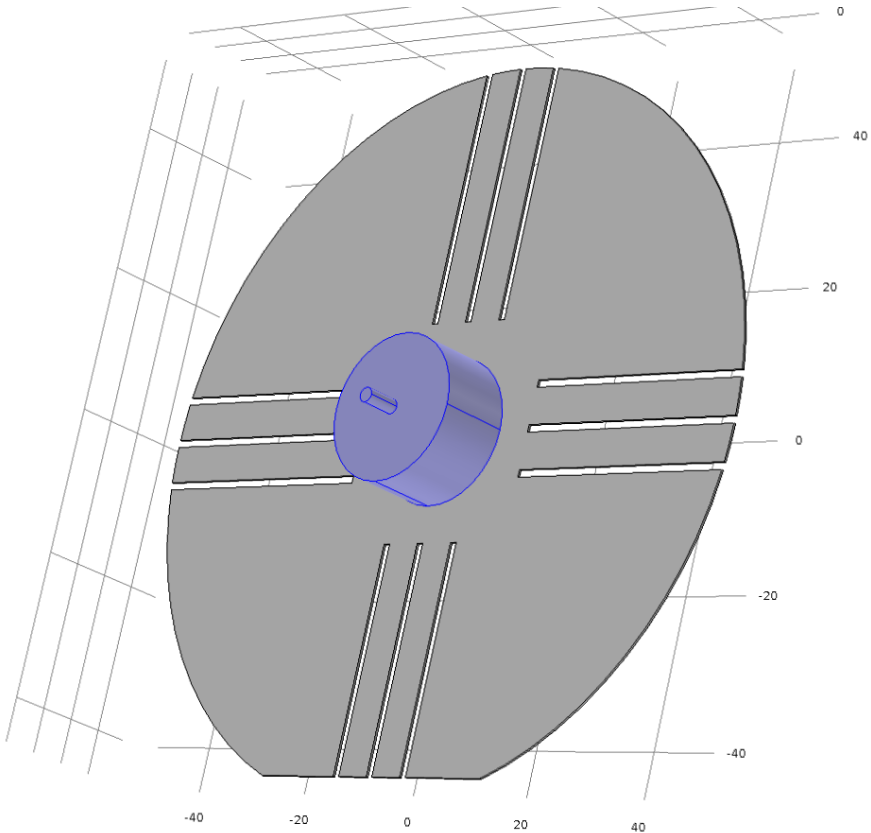


Figure 3: Model 1, back view

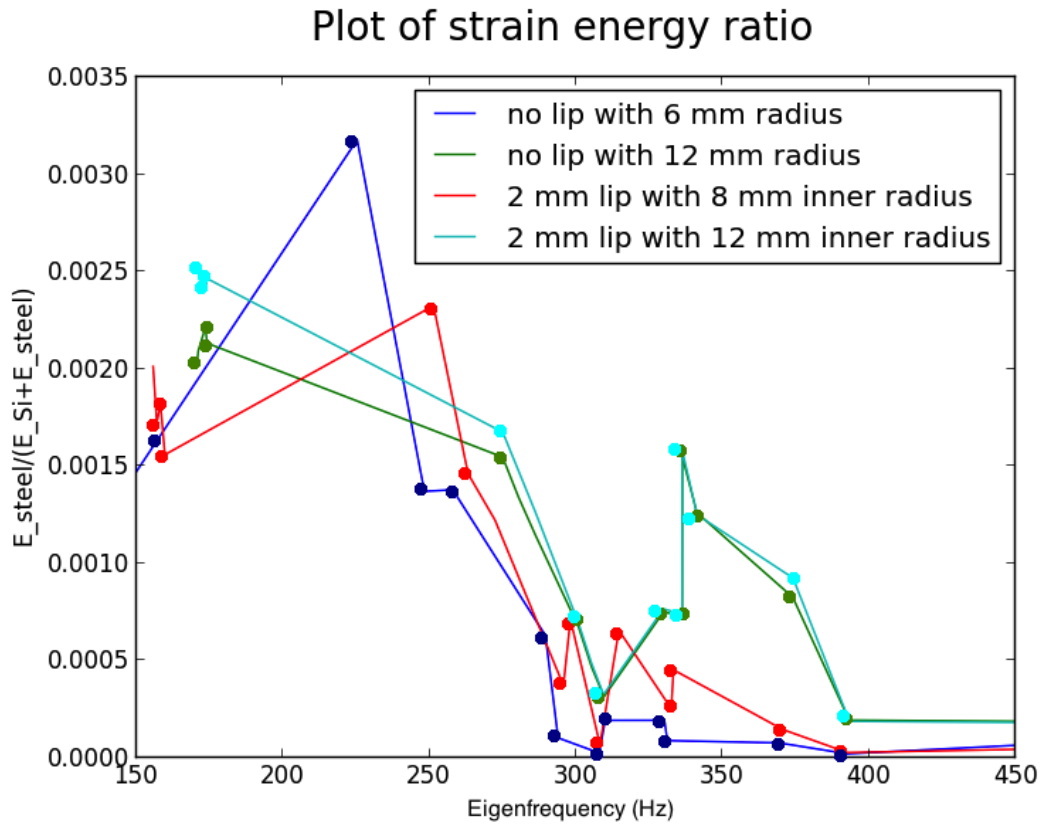


Figure 4: Comparison of strain energy ratio between Models 1 and 3 with varying radii

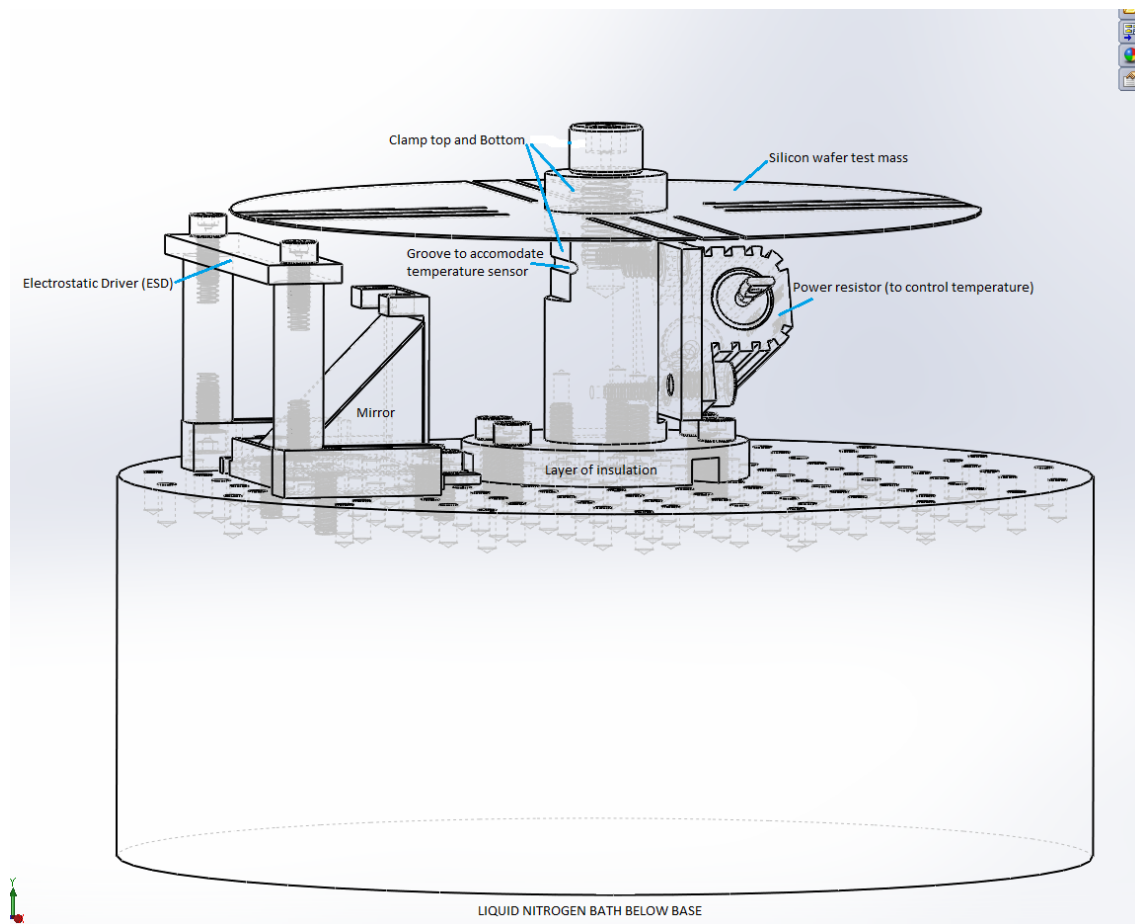


Figure 5: Experimental set-up. The ESD sends electrical pulses that will drive the thin cantilevers in the wafer. Although the base will be at liquid nitrogen temperature, we adjust the temperature of the silicon with the power resistor on the back of the bottom clamp. A laser will come in from the side, reflect off of the mirror onto the oscillating cantilever and bounce back to a quadrant photodetector

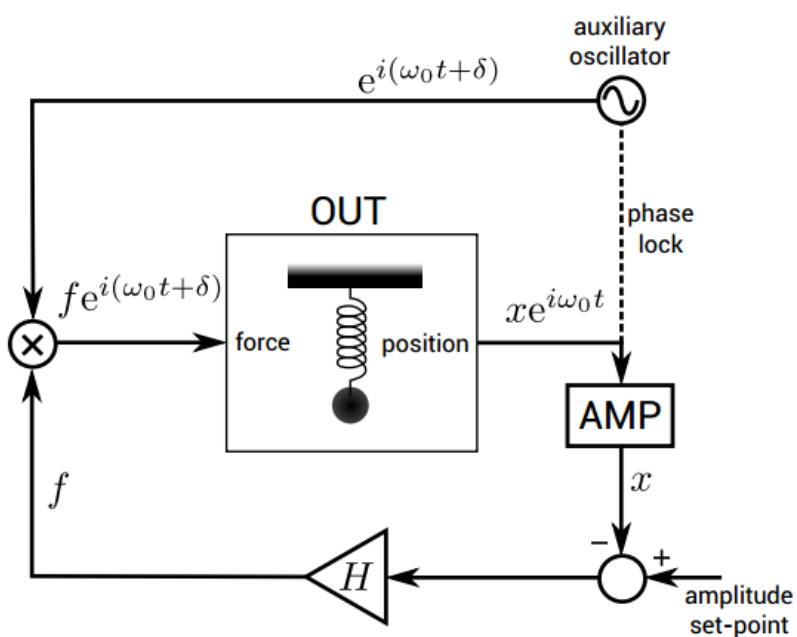


Figure 6: Block diagram of driving system. The oscillator under test (OUT) is driven by an auxiliary oscillator phase locked to the position signal. The amplitude is detected using an amplitude detector, labeled AMP. The amplitude is controlled by an amplitude locked loop (ALL).

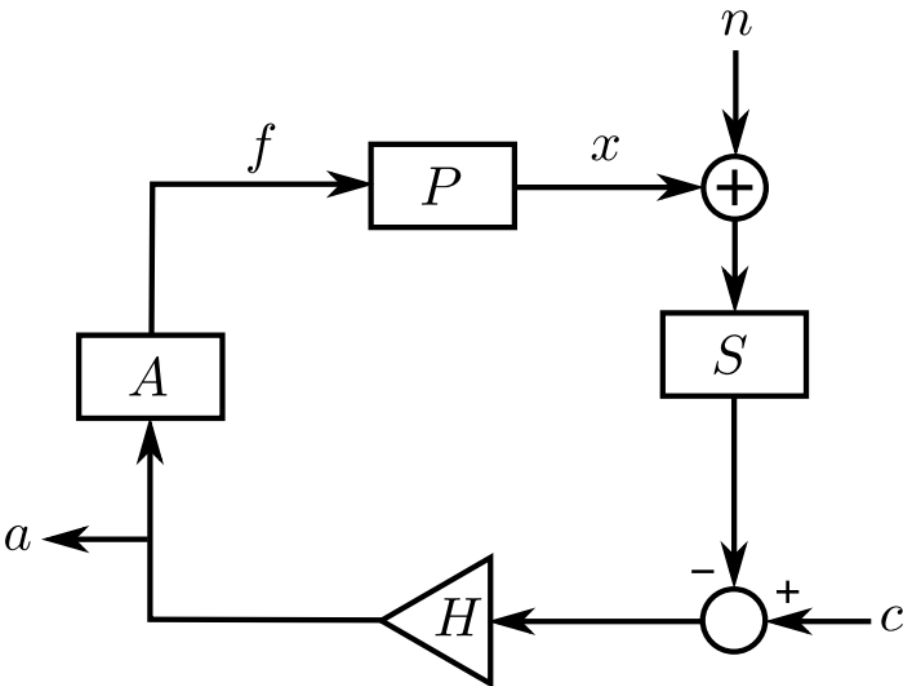


Figure 7: Linearized block diagram of the amplitude locked loop.

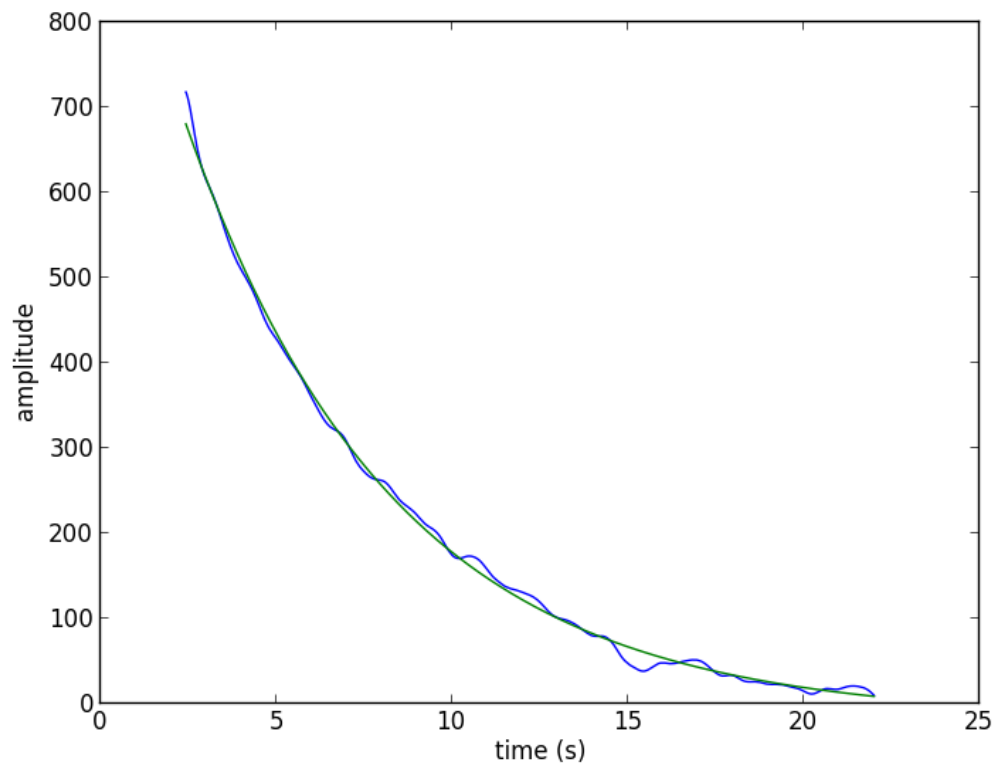


Figure 8: Green line is the curvefit of the exponential ringdown. Here we have extracted all of the local minima of the exponential decay curve, resulting in the blue line of data.

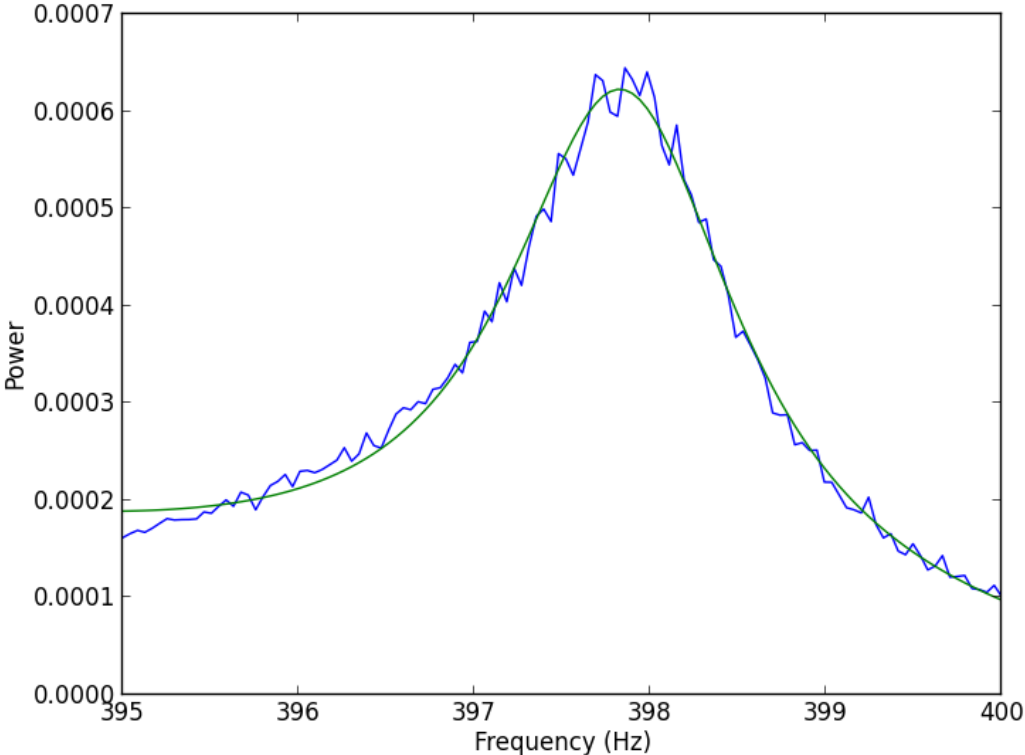


Figure 9: Green line is the curvefit of the transfer function.

Tables

| Trial # | Method | Q with error |
|---------|-------------------|-----------------|
| 1 | Ringdown | 371.0 ± 0.8 |
| 2 | Ringdown | $355.4 \pm .7$ |
| 3 | Transfer Function | 247 ± 4.92 |

Table 1: Measurements of the quality factor of aluminum cantilevers.

References

- [1] Nawrodt, Ronny. "Investigations of mechanical losses of thin silicon flexures at low temperatures." arXiv, 15 Mar. 2010. Web.28 Apr. 2014. <http://arxiv.org/pdf/1003.2893v1.pdf>.
- [2] Painter, Oskar. "Laser cooling of a nanomechanical oscillator into its quantum ground state." Nature 478(): 89-92, Print.
- [3] Saulson, Peter. "Thermal noise in mechanical experiments." Physical Review D42 (): 2437-2445. Print.
- [4] Veggel, A A Van. "Silicon mirror suspensions for gravitational wave detectors." Classical and Quantum Gravity (): 025017. Print.
- [5] Thanks to my mentors Nicolas Smith-Lefebvre and Zach Korth for their input!